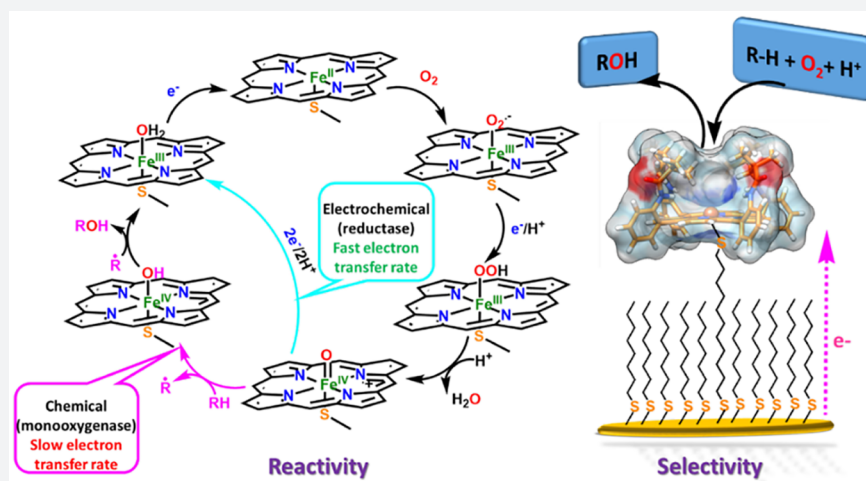


Electron Transfer Control of Reductase versus Monooxygenase: Catalytic C–H Bond Hydroxylation and Alkene Epoxidation by Molecular Oxygen

Manjistha Mukherjee¹ and Abhishek Dey^{1*}

Department of Inorganic Chemistry, Indian Association for the Cultivation of Science, Kolkata, West Bengal, India 700032

Supporting Information



ABSTRACT: Catalytic oxidation of organic substrates, using a green oxidant like O_2 , has been a long-term goal of the scientific community. In nature, these oxidations are performed by metalloenzymes that generate highly oxidizing species from O_2 , which, in turn, can oxidize very stable organic substrates, e.g., mono-/dioxygenases. The same oxidants are produced during O_2 reduction/respiration in the mitochondria but are reduced by electron transfer, i.e., reductases. Iron porphyrin mimics of the active site of cytochrome P450 (Cyt P450) are created atop a self-assembled monolayer covered electrode. The rate of electron transfer from the electrode to the iron porphyrin site is attenuated to derive monooxygenase reactivity from these constructs that otherwise show O_2 reductase activity. Catalytic hydroxylation of strong C–H bonds to alcohol and epoxidation of alkenes, using molecular O_2 (with $^{18}O_2$ incorporation), is demonstrated with turnover numbers $>10^4$. Uniquely, one of the two iron porphyrin catalysts used shows preferential oxidation of 2° C–H bonds of cycloalkanes to alcohols over 3° C–H bonds without overoxidation to ketones. Mechanistic investigations with labeled substrates indicate that a compound I ($Fe^{IV}=O$ bound to a porphyrin cation radical) analogue, formed during O_2 reduction, is the primary oxidant. The selectivity is determined by the shape of the distal pocket of the catalyst, which, in turn, is determined by the substituents on the periphery of the porphyrin macrocycle.

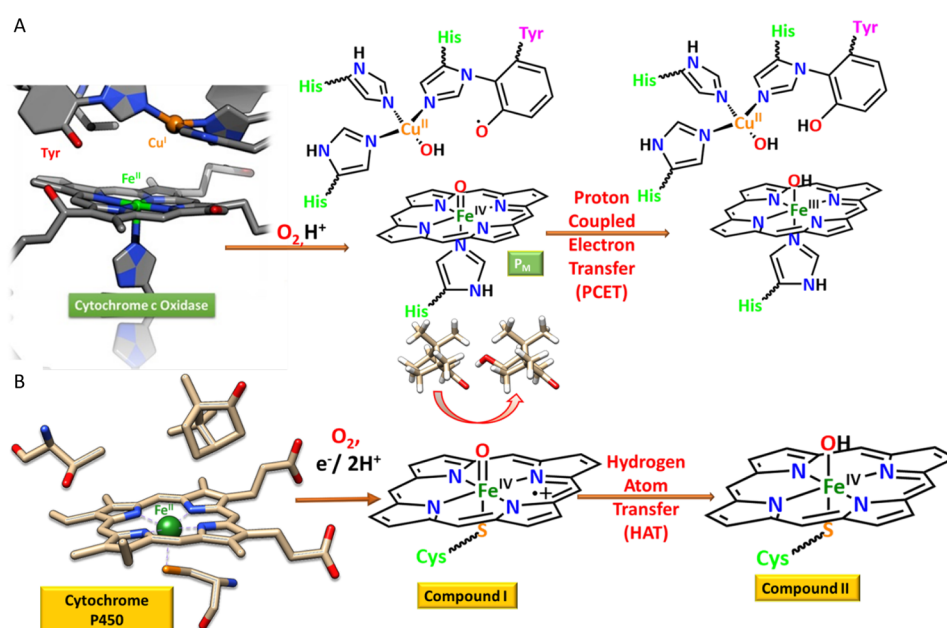
1. INTRODUCTION

Over several decades chemists have been pursuing the development of efficient catalysts for the oxidation of organic substrates using an environmentally benign oxidant like molecular O_2 .^{1–8} Inspiration for the design of these catalysts has been derived from the diverse set of metallo-enzymes that are known to facilitate these transformations under ambient conditions. These include heme (cytochrome P450,^{9–11} indole dioxygenase¹²) and nonheme (intradiol dioxygenase,¹³ methane mono-oxygenase¹⁴) dioxygenases and mono-oxygenases. All of these enzymes have evolved to use iron in the active site and molecular O_2 as the oxidant for both $2e^-$ mono-oxygenation and $4e^-$ dioxygenation.¹³ Organic substrates, which are generally stable in oxygen, are reacted by reactive

high-valent intermediates which are formed upon reacting molecular oxygen with the reduced ferrous sites in these enzymes.^{15–20} The high-valent iron species are formed upon the cleavage of the O–O bond of a ferric peroxide intermediate, which, in turn, is formed after the two-electron reduction of O_2 .^{9,21–24} These high-valent species are either, formally, $Fe(V)=O$ in heme (Scheme 1a,b) or $Fe(IV)=O$ in nonheme iron enzymes. These species are highly oxidizing and can oxidize strong C–H bonds by hydrogen atom abstraction (HAT) as well as oxidize poorly reactive alkenes to epoxides.^{25–37} The generation of the formally $Fe(V)=O$

Received: January 16, 2019

Published: April 3, 2019

Scheme 1. Primary Reactions Taking Place at the Active Site of (A) Cytochrome c Oxidase⁴² and (B) Cytochrome P450⁴³

species in heme systems requires two electrons that are provided by electron transfer (ET) from a reductase component (Scheme 1b).⁹ The reactivity of these species varies dramatically depending on the axial ligands and spin state of the iron among other factors.^{38–40} Alternatively, these high-valent species are also produced in the heme/Cu active site of oxygen reductases like cytochrome c oxidase (Scheme 1a), the terminal oxidant of the mitochondrial electron transport chain, where they are reduced by rapid electron transfer (10^5 s^{-1}) from the adjacent heme b or Cu_A sites present in the same protein. In Cyt P450 mono-oxygenases the electron transfer rates from the reductase component (Scheme 1b) to the heme site varies between 36 s^{-1} and 12 s^{-1} ,⁴¹ which are substantially slower than the electron transfer rates between the heme b/Cu_A and the heme-Cu active site in oxygen reductase like CcO.

Synthetic efforts mimicking the structure and reactivity of these excellent natural catalysts started even before the crystal structures were available for most of these.^{44–48} Mechanistic investigations allowed identifying reactive intermediates responsible for the oxidation of poorly reactive organic molecules. Synthetic analogues of these intermediates were prepared outside the protein matrix which allowed detailed interrogations of these species and provided deep insight into their electronic structure that was responsible for low reaction barriers and selectivity.⁴⁹ The compound I, which is a Fe^{IV}=O bound to a porphyrin radical cation in heme systems (or [Fe^{IV}=O]P⁺), can be directly generated by two-electron oxidation of a Fe(III) center with peroxides and per-acids using the peroxide shunt.^{50–53} Generation of these high-valent species from molecular oxygen in synthetic heme systems still remains a formidable challenge. As a result, the scope of molecular O₂ as a green oxidant in artificial systems remains limited.^{54,55} Though there are number of metal catalysts reported that can oxidize organic molecules in the presence of oxygen, the generation of the free radical species during the course of the reaction makes a huge difference in the oxidation chemistry.⁵⁶ Furthermore, modeling the electron transfer to

synthetic models at intermediate states of catalysis is difficult owing to the inherent reactivity of a sacrificial reductant with O₂. For example, in the case of mono-oxygenases, where a ferric resting site is generated as the end-product of the catalytic cycle, its reduction to the O₂ activating ferrous form is jeopardized by the reaction of O₂ with reducing agents present in the medium.

Apart from some photocatalysts,⁵⁷ recently some reports have been published that demonstrate different metal porphyrins that can oxidize cycloalkanes^{58–60} and alkenes^{61–65} under homogeneous conditions at high temperature and high pressure of oxygen with low turnover numbers and no selectivity. Similarly, synthetic mimics of O₂ reducing proteins like cytochrome c oxidase are reported to oxidize organic phosphines using molecular O₂, albeit under single turnover conditions in organic solvents; i.e., these artificial oxidants are potent but not catalytic.^{66,67} Reductive activation of molecular oxygen to generate high-valent species that could oxidize organic substrate was demonstrated using a biphasic medium where Mn porphyrins were dissolved in organic solvent that also contained the organic substrate, and the reducing equivalents were provided from ascorbic acid present in the aqueous phase. Catalytic rates of 0.6 per hour and 0.04 per hour could be reached for oxidation of styrene to styrene oxide and cyclohexane to cyclohexanol, respectively.⁶⁸

In this manuscript, thiolate bound iron-picket fence porphyrin (FePf) assembled over self-assembled monolayer (SAM) is used to create an electrochemical analogue of cytochrome P450 to generate high-valent oxidants during heterogeneous electrochemical O₂ reduction. The rate of electron transfer from the electrode to the catalyst is attenuated to enhance the lifetime of these high-valent species which could, thus, be used to oxidize C–H bonds and epoxidize alkenes catalytically using O₂ with turnover numbers greater than 10⁴. The sterically hindered distal pocket of the picket fence porphyrin allows easy access to the sterically less hindered 2° C–H bonds relative to the 3° C–H bond and

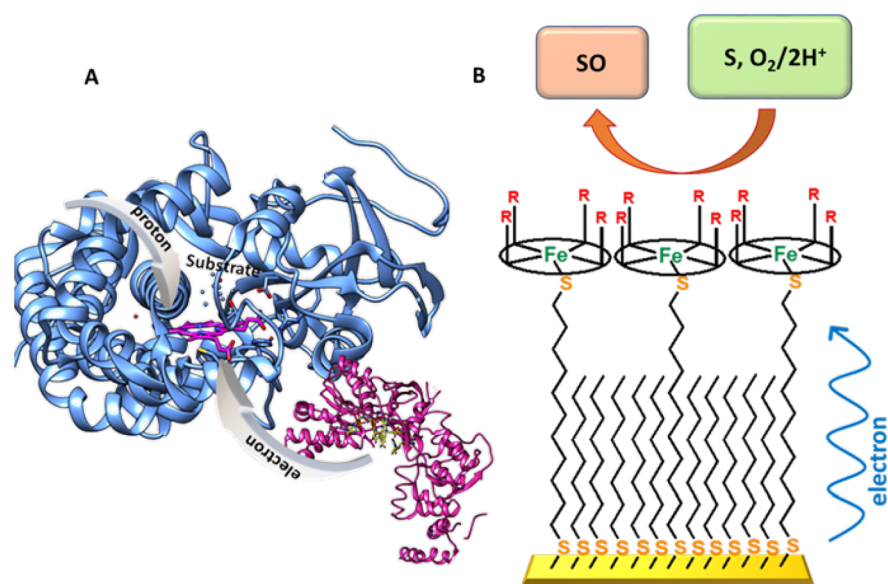


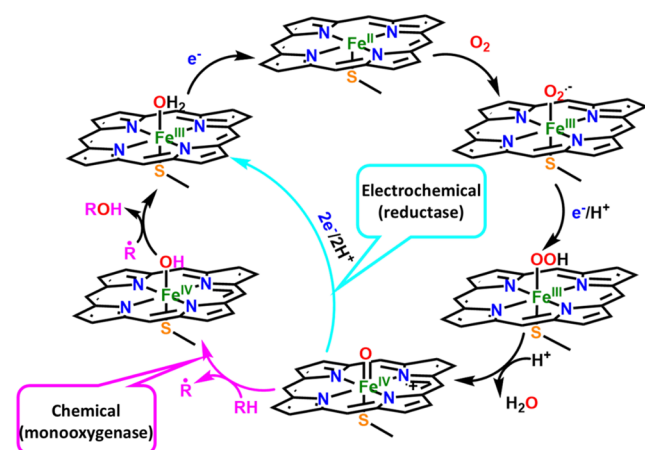
Figure 1. Graphical representation of (A) the cytochrome P450 reductase system and (B) the electrochemical analogue.

shows no overoxidation of alcohols to ketones for sterically hindered alcohols.

2. AN ELECTROCHEMICAL MODEL OF CYTOCHROME P450

The key toward generating high-valent oxidant from oxygen is retarding the rate of ET from the reductase component to the catalytic center (Figure 1A) to allow mono-oxygenase activity in preference to reductase activity (Scheme 2). In fact, several

Scheme 2. Schematic Representation of the Oxidation of Small Organic Molecules by the High-Valent Iron Species, Formed during the Reduction of Oxygen by the Synthetic Iron Porphyrin Complexes



reactive intermediates are now known to accumulate on the electrode during heterogeneous electrochemical oxygen reduction under steady state (Scheme 2). This includes $\text{Fe}^{\text{III}}\text{-OOH}$, $\text{Fe}^{\text{IV}}\text{=O}$, and in some cases $[\text{Fe}^{\text{IV}}\text{=O}]\text{P}^+$.^{69–73} This is because an electrocatalytic O_2 reduction (reductase activity) involves the same intermediates (Scheme 2) that are involved in substrate oxidation (oxidase reactivity) even in artificial systems as well. The only difference is that during

electrocatalytic O_2 reduction the high-valent oxidants are reduced by ET from the electrode, which acts as a mimic of the reductase component in the enzymatic systems (Figure 1B). This raises the possibility of harnessing the oxidase activity of these high-valent intermediates to oxidize organic molecules if their rates of formation via O–O heterolysis during O_2 activation can be made much faster than their rates of decay (by electron transfer from the electrode, Figure 1B), offering them substantial lifetime to oxidize substrates present in the medium. Recent efforts have demonstrated that the rate of O–O bond cleavage by an iron porphyrin complex, during electrocatalytic O_2 reduction, can be substantially enhanced by using a thiolate as an axial ligand.⁷¹ The strong iron thiolate bond ($\text{Fe-S} = 341 \text{ cm}^{-1}$ in the surface enhanced resonance Raman spectroscopy (SERRS) spectra obtained on these modified electrodes) activates the O–O bond for cleavage by exerting a “push” effect.⁴³ Similarly, the rate of electron transfer from the electrode to the electrocatalytic center can be attenuated by the use of SAM of thiols on electrodes.^{74–76} Combining both, one can envisage an electrochemical construct where reactive oxidants are produced atop electrodes during O_2 reduction and may have substantial lifetime to oxidize organic molecules present in the solution (Figure 1). Preliminary data showing successful oxidation of poorly reactive hydrocarbons and ferrocyanide using high-valent intermediates produced during electrochemical reduction of molecular O_2 utilizing this approach were reported a few years back.^{71,77}

3. OXIDATION OF THE SUBSTRATES

A thiolate bound iron-picket fence porphyrin (FePf, Figure 2A) has a $E_{1/2} = -51 \text{ mV}$ vs NHE for the $\text{Fe}(\text{III})/\text{Fe}(\text{II})$ redox pair at pH 7 and reduces O_2 at cathodic potentials (Figure S.1) with a maximum current at -201 mV vs NHE.⁷¹ In the presence of dissolved organic substrates in water, bulk electrolysis at -100 mV for 15 min yields oxidized products which are then extracted in an organic solvent and analyzed using GC-MS. Catalytic hydroxylation of $\text{sp}^3 \text{ C-H}$ bond of a cyclohexane and epoxidation of styrene could be achieved using molecular O_2 with large turnover numbers (TONs) and

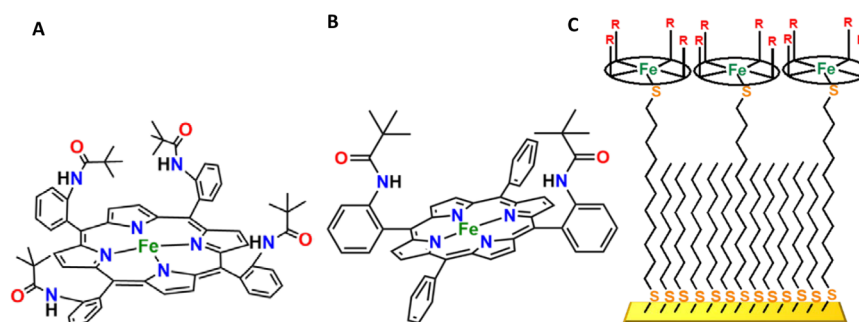


Figure 2. Catalysts used in the reactions (A) iron-picket fence porphyrin (FePf) and (B) iron-half picket fence porphyrin (FehPf). (C) The modified electrode with thiolate ligated iron porphyrin.

Table 1. Turnover Numbers (TONs), Turnover Frequencies (TOFs), and the Amount of $^{18}\text{O}_2$ Incorporation in the Products Obtained after the Oxidation of Substrates by Thiolate Ligated FePf Complex

| Substrate BDE (kCal/mole) | Oxidized Product | Turn Over Number (TON) | Turn Over frequency (TOF) (sec^{-1}) | ^{18}O inclusion |
|--|------------------|---------------------------|---|---------------------------|
| (100) | | 2.1×10^4 | 23 | 100% |
| | | 5.7×10^3 | 6 | 60% |
| ($1^\circ \text{C-H} = 98$) ($2^\circ \text{C-H} = 85$) | | 2.17×10^4 | 24 | ND |
| | | 6.9×10^3 | 8 | |
| (89.8) | | 8.62×10^2 | 1 | 100% |
| | | 6.11×10^4 | 68 | 0% |

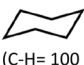
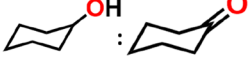
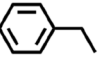
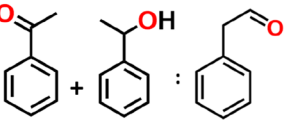

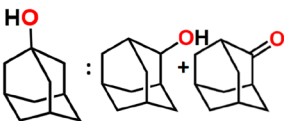
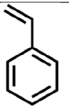
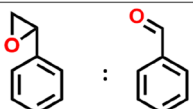
high turnover frequencies (TOFs) (Table 1) with a thiolate bound FePf. Oxidation of cyclohexane leads exclusively to cyclohexanol with $\text{TON} > 10^4$ and $\text{TOF} \sim 23 \text{ s}^{-1}$. Note that these are rates averaged over the entire reaction time. Similarly, styrene is oxidized to styrene oxide with a $\text{TON} > 10^3$ and $\text{TOF} \sim 6 \text{ s}^{-1}$. Generally, epoxidation by high-valent ferryl species is faster than C–H hydroxylation. Thus, the slower rate of epoxidation may reflect lower solubility or steric demand of the styrene substrate (see section 3.3). Ethylbenzene gets oxidized to produce a 3:1 mixture of acetophenone and phenylacetaldehyde, and toluene gets oxidized to benzaldehyde (Table 1). Oxidation of primary C–H bonds in the presence of benzylic C–H bonds in ethylbenzene is very uncommon and reflects steric hindrance in the distal pocket (see section 3.3). Thus, the thiolate bound iron porphyrin created on top of an electrode is a functional mimic of the cytP450-reductase system and can catalyze both hydroxylation and epoxidation of organic substrates with O_2 akin to its natural analogue.

3.1. Molecular Oxygen Incorporation. The incorporation of molecular O_2 in the product was confirmed by

labeling experiments using labeled $^{18}\text{O}_2$. Labeling the molecular O_2 using $^{18}\text{O}_2$ resulted in labeled cyclohexanol (100%) and styrene oxide (60%) (Table 1, Figure S.2). The partial labeling of styrene oxide, which is produced at a slower rate (Table 1), is suggestive of competitive oxygen atom exchange of a high-valent metal oxo species with unlabeled water.⁷⁸ Thus, the oxygen atoms incorporated in the product are obtained from the O_2 establishing catalytic monooxygenase activity. None of the aldehyde produced is found to be labeled with ^{18}O as the rate of exchange of the aldehyde oxygen with unlabeled water is $\sim 10^5 \text{ M}^{-1} \text{ s}^{-1}$ in buffered solutions.⁷⁹

3.2. Regioselectivity. Upon using a substrate like adamantane which bears both 2° and 3° aliphatic C–H bonds with BDEs of 100.2 kcal/mol and 97 kcal/mol, respectively, the 2° alcohol is observed as the major product, even after considering the statistical probability,⁸⁰ resulting in a 3° and 2° ratio of 0.68 (Table 2). Most known metal oxo ligands produce the 3° alcohol as a dominant product ($3^\circ:2^\circ > 48:1$ for cyt P450 and other heme systems⁸¹) consistent with

Table 2. Regioselectivity for Two Different Porphyrins

| Substrate | Oxidized Product | Product Distribution for two different catalysts | |
|--|---|--|--|
| | | FePf | FehPf |
|  (C-H = 100 kcal/mol) |  | Only Cyclohexanol | 2.6:1 (only cyclohexanone on longer runs) |
|  (1° C-H = 98 kcal/mol) (2° C-H = 85 kcal/mol) |  | 3:1 | No 1° oxidation product. Only benzylic C-H oxidation observed. |
|  (2° C-H = 100 kcal/mol) (3° C-H = 97 kcal/mol) |  | 2:3 (No Adamantanone) | 4:1 (ratio of adamantane-2-ol and adamantanone is 1:2) |
|  |  | Only styrene oxide | 62:1 (4.4 times more styrene oxide) |

the weaker BDE of 3° sp³ C–H bonds.⁸⁰ Similarly, upon using ethylbenzene the 1° C–H bond (BDE = 98 kcal/mol) and the benzylic C–H (BDE = 85 kcal/mol) bond are oxidized to yield phenyl acetone and acetophenone, respectively. Generally, oxidation of primary C–H in the presence of weak benzylic C–H is not observed.²³ Thus, observation of primary C–H oxidation in the presence of benzylic C–H is indeed quite remarkable. Overoxidation of the alcohol to the aldehyde is observed in the case of the less sterically crowded primary and benzylic C–H bonds in ethylbenzene and toluene (Table 1, rows 3 and 4). Importantly, in the case of sterically demanding substrate like cyclohexane or adamantane, no cyclohexanone or adamantanone is detected. The apparent disparity with the erstwhile reported synthetic systems regarding the preferential oxidation of 2° C–H over 3° C–H and lack of overoxidation of the sterically demanding 2° alcohol produced all suggest that steric demands of the picket fence architecture may be responsible for the regioselectivity observed here.

To ascertain the role of steric demand of the picket fence architecture in selectivity, an iron-half picket fence porphyrin (FehPf, Figure 2B) is synthesized, which has two bulky pivaloyl groups in the distal site in contrast to four in the picket fence architecture which allows more rotational flexibility to the pivaloyl groups. Catalysis was performed using the FehPf, which has a wider substrate access cavity, keeping everything else the same. The results show that cyclohexanol and cyclohexanone are produced during the oxidation of cyclohexane with the ratio of 2.6:1 in contrast to only cyclohexanol with FePf (Table 2, S.I. Figure S.3.A). The cyclohexanone is the only product when the reaction is run longer to higher conversion, indicating that the ketone produced was the result of overoxidation of the alcohol. With ethyl benzene there is no trace of primary aliphatic C–H hydroxylation, and only benzylic oxidation is observed as is known to be the case for

most systems reported to date (Table 2, S.I. Figure S.3.B). Similarly, the 4:1 ratio of the 3°:2° product for adamantane hydroxylation along with the production of adamantanone due to overoxidation of the 2° alcohol (Table 2, S.I. Figure S.3.C) validates the proposal of steric control of selectivity in FePf. Moreover, the TOF of styrene epoxidation with FehPf is four times higher than that obtained with FePf (Table 2, S.I. Figure S.3.D), suggesting that the sluggish rate of styrene epoxidation observed with FePf is the consequence of the sterically demanding architecture of the picket fence providing limited access of the alkene (side-on) groups of styrene.

The four pivaloyl groups of picket fence around the porphyrin ring on the distal side (the proximal side is thiolate bound and faces the SAM) has an opening of ~6 Å (Figure 3A), which may restrict the access of sterically demanding 3° C–H. Access of the tertiary C–H bonds of adamantane to the high-valent ferryl center buried deep inside the pocket is to be more demanding (Figure 3B) relative to the access of the 2° C–H (Figure 3C). This may result in the higher rate of oxidation of 2° C–H in adamantane relative to the weaker 3° C–H observed here. Similarly, the picket fence architecture can allow unabated preferential access to the terminal –CH₃ group of ethylbenzene. As a result, while the benzylic hydroxylation and aromatic hydroxylation are much more usual for ethylbenzene oxidation,²³ here a substantial amount of primary aliphatic C–H bond oxidation is observed despite having a much higher BDE than the benzylic C–H bond. The α-H of a 2° alcohol generated upon the oxidation of 2° C–H in cyclohexane and adamantane is effectively a 3° center. Therefore, no overoxidation is observed in these cases. Thus, the steric hindrance of the distal pocket of the iron picket fence porphyrin seems to allow for (a) preferential 2° C–H hydroxylation in adamantane, (b) primary C–H oxidation in ethylbenzene, and (c) lack of overoxidation of 2° alcohols. The FehPf architecture on the other hand is open, allowing easy

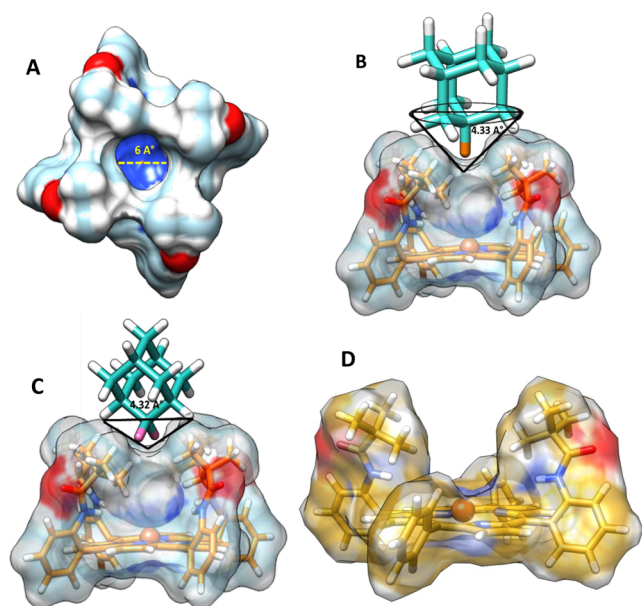
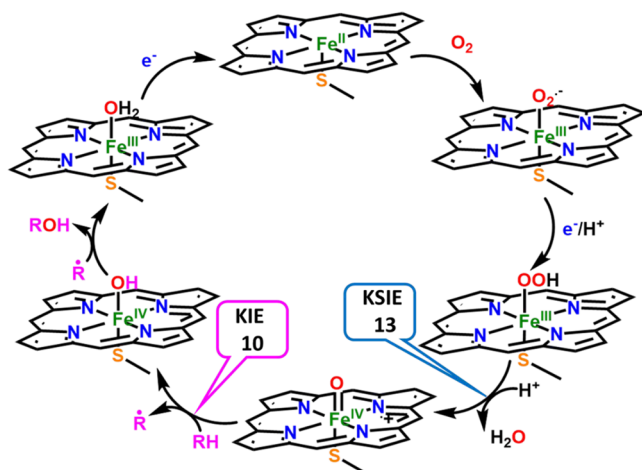


Figure 3. (A) Top view of FePf showing a substrate access cavity with a diameter of 6 Å. (B) The access of 3° H of adamantane demands a conelike geometry resulting in steric hindrance, (C) secondary C–H accesses to the cavity with a lesser steric hindrance because of its trigonal architecture resulting in higher yields of secondary alcohol, and (D) wider substrate access cavity of iron-half picket fence (FehPf) depicting the lesser amount of bulky pivaloyl groups in the secondary geometry.

access to sterically hindered substrates which compromises the selectivity (Figure 3D).

3.3. Isotope Effect. H/D isotope effects were obtained for cyclohexane- d_{12} . The H/D isotope effect for cyclohexane (sp^3 C–H) is measured to be 9.9 ± 0.3 . The values of KIE fall in the observed range expected for rate determining HAT reactions (Scheme 3).^{82,83} Several cytP450 are known to exhibit k_H/k_D as high as 10 for HAT by compound I.^{84–87} These reactions are performed in an aqueous medium, providing a unique opportunity to explore the H_2O/D_2O

Scheme 3. Schematic Representation of the Mono-oxygenase Activity Depicting Both the Kinetic Solvent Isotope Effect (KSIE) and Kinetic Isotope Effect (KIE) during the Oxygenation of C–H Bond



solvent kinetic isotope effect (KSIE) in these reactions. The oxidation of cyclohexane by oxygen catalyzed by a thiolate bound iron porphyrin has a H_2O/D_2O isotope effect of 12.8 ± 0.1 . Since a HAT by a high-valent oxo species is not expected to have significant KSIEs, the large KSIE observed here is suggestive of the presence of an exchangeable proton in the transition state of another chemical step in the catalytic cycle (Scheme 3). The CytP450 enzymes exhibit both KSIE (from solvent) and KIE (from substrate) in the same catalytic cycle as has been observed here. The KSIE in cytochrome P450 originates from the protonation of Fe^{III} -peroxide or Fe^{III} -hydroperoxide species,⁸⁸ and the KIE originates from the C–H bond abstraction by compound I.⁴³ Note that observation of isotope effects in two different steps in the same catalytic cycle implies that the rate of O–O bond heterolysis of compound 0 and C–H bond abstraction by compound I are similar (ca. $10\,000\ s^{-1}$).⁴² In a previous investigation, a combination of surface enhanced resonance Raman spectroscopy coupled to rotating disc electrochemistry (SERRS-RDE) and H/D isotope effects on rate-determining steps in O_2 reduction, a KSIE of ~ 18 was observed for an iron porphyrin complex with a covalently bound thiolate.⁸⁹ The large KSIE was associated with the heterolytic cleavage of the O–O bond in a Fe^{III} -OOH intermediate owing to a lack of organized proton transfer channel, which is present in the active site of Cyt P450 comprising of Asp 251 and Thr 252. In fact, large KSIE (~ 10) is observed on the protonation of compound 0 (thiolate bound Fe^{III} -OOH) intermediate in P450 when the preorganized proton transfer channel created by Asp 251 is replaced by Asn.^{90,91}

3.4. Faradaic Yield. Apart from obtaining the TON and TOF, the overall charge dissipated during the electrolysis can be quantified as well and compared to the amount of oxidized product allowing estimation of the Faradaic yield (FY) of the process. The FY helps to quantify the competition between the chemical oxidation step (mono-oxygenase pathway, Scheme 2) by the high-valent oxidant and its reduction by ET from the electrode (reductase pathway, Scheme 2). For example, if the ET from the electrode is sufficiently slow and all the compound I produced catalyzes mono-oxygenation (a 2e-oxidation), one mole of the substrate is oxidized per two moles of electrons provided from the electrode. This situation is defined to have a 100% FY, i.e., the maximum substrate oxidation possible per two electrons from the electrode. The oxidation of cyclohexane to cyclohexanol has a FY of 72%, and the oxidation of styrene to styrene oxide has an efficiency of 45% (Table 3). An efficiency less than 100% is expected, considering the competing reduction of these highly oxidizing species by electron transfer from the electrode which is poised at potentials ($-100\ mV$ vs NHE) that are much lower than the reduction potentials of the oxidant compound I species (generally $\sim 1.3\ V$ vs NHE at pH 6).^{92,93} Since both these experiments are performed at the same potential ($-100\ mV$ vs NHE), the rate of ET from the electrode to the oxidant should be very similar. Thus, the differences in the FY of cyclohexane and styrene oxidation reflect the relative rates of mono-oxygenation and ET in both cases. The FY values indicate that roughly the rate of ET on an octane thiol SAM is the same as the rate of epoxidation of styrene (FY $\approx 45\%$) and is ~ 3 times slower than the rate of hydroxylation of cyclohexane (FY $\approx 72\%$).

The rate of electron transfer from an electrode which is modified with self-assembled monolayers of alkane thiol

Table 3. FY for Cyclohexane and Styrene Oxidation with the Variation of Rate of Electron Transfer from Electrode

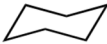

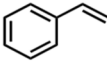
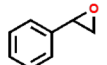


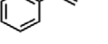
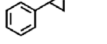
| Substrate | Product | Catalyst | FY (%) for different chain length of the diluent | | | |
|---|---|----------|--|-------------------|-------------------|-------------------|
| | | | C ₁₀ SH | C ₈ SH | C ₆ SH | C ₄ SH |
|  |  | FePf | 56.4 | 72 | 52.1 | 21.0 |
|  |  | FePf | 19.1 | 45 | 21.0 | 12.6 |

Table 4. FY for Cyclohexane and Styrene Oxidation with the Varying Coverage of the Catalyst

| Substrate | Product | FY (%) for different surface coverage of the catalyst | | |
|---|---|---|-----|------|
| | | 10% | 20% | 30% |
|  |  | 29.7 | 72 | 58.4 |
|  |  | 8.4 | 45 | 26.4 |

depends on the chain length of the alkane thiols^{75,94} and the rate decays exponentially with an increase in chain length.⁷⁴ The electrodes used here are modified with linker molecules (SHC₁₁SH) and diluent molecules (C₈SH) where the standard rate of electron transfer is 1000 s⁻¹.^{74,95} An increase in the rate of ET should reduce the lifetime of high-valent species, which should result in a decrease in the FY. Indeed, when the diluent is changed to hexane thiol (C₆SH) and butanethiol (C₄SH), which should have a much larger electron tunneling rate,⁷⁴ the FY of cyclohexane oxidation decreases to 52.1% and 21%, respectively, from 72% in octane thiol (Table 3). Similarly, the FY of epoxidation decreases from 45% in octane thiol to 21% and 12.6% in hexane thiol and butanethiol (Table 3), respectively. The rate of electron transfer can be enhanced by increasing the driving force of electron transfer by applying a more cathodic potential. As may be expected, the yield of oxidized product was reduced dramatically as the applied potential is made more cathodic (S.I., Figure S.4), which results in a higher driving force for electron transfer. Decreasing the rate of ET further by elongating the chain length by substituting octane thiol by decanethiol leads to a decrease in FY as well (Table 1), suggesting that the octane thiol provides an optimal ET rate for the desired mono-oxygenase activity. The abundance of the active site can be controlled by varying the mixture of the linker dithiol with the filler thiol (diluent). The catalytic turnover gradually increases from 10% to 20% coverage and then decreases as the coverage is increased to 30% (Table 4). Thus a 20% coverage of the catalyst is optimal for the reactivity.

During O₂ reduction, this thiolate bound FePf porphyrin produces ~10% H₂O₂.⁹⁶ H₂O₂ is known to produce compound I upon reacting with ferric porphyrins, albeit not bound to thiolate. Oxidation of substrates by compound I produced from the H₂O₂ generated in situ during O₂ reduction will result in a maximum FY of 10% and not as high as 71% observed here. Additionally, the oxidation of cyclohexane by same construct, i.e., thiolate bound FePf, is only observed at 50 mM concentration of H₂O₂. Thus, the likelihood of compound

I formed from H₂O₂ produced under these conditions (0.2 mM O₂) oxidizing substrate is very unlikely.

4. CONCLUSION

In summary, an electrochemical analogue of Cyt P450 is generated by creating thiolate bound iron porphyrin active sites on top of self-assembled monolayer covered electrodes. A highly oxidizing species is produced during the catalytic O₂ reduction cycle which can be used to catalytically oxidize cyclohexane and styrene to cyclohexanol and styrene epoxide, respectively, with TON > 10⁴ and TOF 6–23 s⁻¹. A large KIE (10) and KSIE (13) indicate that a Fe^{III}-OOH species, generated during O₂ reduction, undergoes heterolytic O–O bond cleavage to form a compound I analogue which performs the hydroxylation via HAT. The design of the distal site of the porphyrin used here determines the regioselectivity. In fact, by using a sterically demanding picket fence distal site of the porphyrin ligand, preferential oxidation of 2° C–H bond hydroxylation over 3° C–H bond is observed, and over-oxidation of the alcohol produced could be avoided. The best yields require optimal ET rates (controlled by chain length of the SAM and applied potential) and optimal catalyst coverage (controlled by mole fraction of the ligating dithiol) and TON of 23 000 and FY as high as 70% has been observed for the oxidation of cyclohexane to cyclohexanol. Overall it is demonstrated that the reactivity of electrodes bearing thiolate bound iron porphyrin could be switched between O₂ reductase and mono-oxygenase by controlling the rate of electron transfer from the electrode. The approach demonstrated here has the potential of being applied to other organic molecules specifically to water-soluble natural products of their precursors where such selective hydroxylation has valuable implications.

5. EXPERIMENTAL PROCEDURES

5.1. Materials. All reagents were of the highest grade commercially available and were used without further purification. Octanethiol (C₈SH), butanethiol (C₄SH), potas-

sium hexafluorophosphate (KPF₆), benzyl alcohol, benzaldehyde, styrene, styrene oxide, adamantane, and phenylacetaldehyde were purchased from Sigma-Aldrich. Disodium hydrogen phosphate dihydrate (Na₂HPO₄·2H₂O), cyclohexane, and cyclohexanol were purchased from Merck. Triethylamine (Et₃N), toluene, ethylbenzene, and acetophenone were purchased from Spectrochem India Ltd. Au wafers were purchased from Platypus Technologies (1000 Å of Au on 50 Å of Ti adhesion layer on top of a Si(III) surface). The picket fence iron porphyrin was synthesized and characterized following past literature reports.⁹⁷

5.2. Instrumentation. All electrochemical experiments were done using CH Instruments (model CHI700E electrochemical analyzer). The bipotentiostat, Ag/AgCl/KCl (satd.) reference electrodes, and Teflon plate material evaluating cell (ALS Japan) were purchased from CH Instruments. All qualitative and quantitative experiments were done using a gas chromatography mass spectroscopy (GC-MS) technique in an Agilent 7890B GC system with 5977A MS detector.

5.3. Construction of the Electrode. **5.3.1. Formation of Mixed SAM.** The Au wafers were cleaned electrochemically by sweeping several times between 1.7 V to -0.3 V (vs Ag/AgCl reference electrode) in 0.5 M H₂SO₄. A SAM solution was prepared using the proper concentration ratio of the linker (SHC₁₁SH) molecules and the diluent molecules (Figure 4).



Figure 4. Panel (A) is the linker (SHC₁₁SH) and (B) represents the diluent molecules ($n = 1, 3, 5, 7$ respectively for C₄SH, C₆SH, C₈SH, and C₁₀SH).

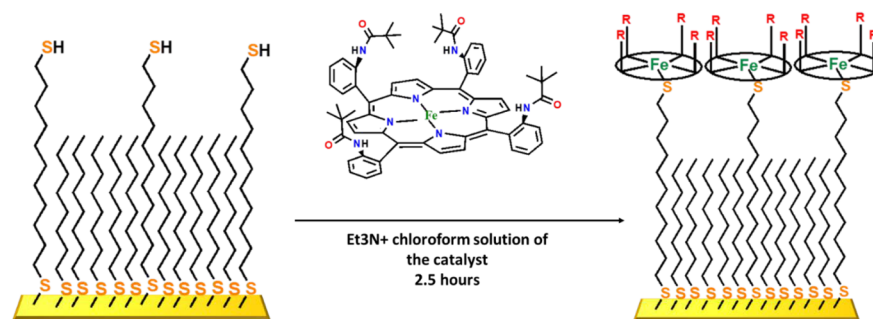
In this SAM solution, the total thiol concentration was maintained to 3 mM, and the mole fraction of the linker thiol was maintained at 0.2 (20%) because that is the optimal concentration for the reactivity. The linker molecule was

prepared using a reported procedure.⁷¹ Octanethiol was used as the diluent in all the experiments performed except in the experiments where the rate of electron transfer was either accelerated by using shorter butanethiol and hexanethiol or decelerated by using longer decanethiol.⁹⁸ Freshly cleaned Au wafers were rinsed with triple distilled water and ethanol. After that, the wafers were purged with dry N₂ gas and immersed in the depositing solution for 48 h.

5.3.2. Attachment of the Catalyst to the Electrode. Au wafers immersed in the deposition solution were taken out before experiments and rinsed with ethanol followed by triple distilled deionized water and then dried under N₂/Ar gas. The wafers were then inserted inside a Plate Material Evaluating Cell (ALS Japan). Primarily, iron porphyrin with a hydrophobic distal pocket (iron-picket fence porphyrin, FePf) was used as catalyst. Along with this, another iron porphyrin with less sterically demanding architecture, iron-half picket fence, was also used as the catalyst. Both the catalysts were dissolved in chloroform for attachment. For the attachment of the iron-picket fence (FePf) to the SHC₁₁SH linker, the electrode surfaces were immersed first in Et₃N for 10 min and then in the iron-picket fence porphyrin solution for 2.5 h (Scheme 4). After that, the surfaces were thoroughly rinsed with chloroform, ethanol, and triple distilled water before the electrochemical experiments. A pH 7 buffer solution containing 100 mM Na₂HPO₄ and 100 mM KPF₆ (supporting electrolyte), Pt wire as counter electrode, and Ag/AgCl as the reference electrode were used for all electrochemical experiments. Cyclic voltammetry (CV) and X-ray photoelectron spectroscopy (XPS) were performed to characterize the catalyst attached to the SAM coated gold electrode (S.I., Figure S.5.1 and S.5.2). Attachment of the FePf on top the SAM modified gold electrode was done following the same technique. The synthetic procedure of Fe-half picket fence is mentioned in the Supporting Information (S.I., S.6).

5.4. Oxidation of Substrates. Substrates used here were cyclohexane, styrene, ethylbenzene, toluene, and adamantane. A pH 7 phosphate buffer solution (deionized water solution containing 100 mM Na₂HPO₄·2H₂O and 100 mM electrolyte, KPF₆) was saturated with the above-mentioned substrates by adding two drops of ethanol to a suspension of these organic molecules in water followed by vigorous shaking. The mixture settled until the aqueous and organic phases were clear. The aqueous layer was separated using a separating flask. Electrochemical analyses were performed with this aqueous solution (S.I., Figure S.7.A). Electrolysis was performed at a constant potential of -0.100 V (vs NHE) (S.I., Figure S.7.C)

Scheme 4. Schematic Representation of the Construction of Bioinspired Electrodes^a



^aCatalyst, iron-picket fence porphyrin (FePf), attached on top of the SAM coated gold electrode.

with this solution for 15 min. CV data collected after bulk electrolysis (S.I., Figure S.7.B) indicate the decay of the catalysts during electrolysis. The resultant aqueous electrolyte containing reactants and products was extracted with chloroform (CHCl₃). The CHCl₃ layer was dried and evaporated, and the product left behind was subjected to GC-MS analysis (S.I., Figure S.8). Note that ethanol used here to make the substrates more soluble in water acts as a competing substrate in this reaction as acetaldehyde was detected in GC. However, the amount is low owing to its higher solubility in water and lower affinity for the hydrophobic electrode surface.

5.5. Labeling with Molecular Oxygen. To calculate the amount of molecular oxygen inclusion, a labeling experiment with ¹⁸O₂ was performed. A degassed pH 7 phosphate buffer, saturated with substrates, was taken and followed by saturating this buffer with ¹⁸O₂. Electrocatlysis was performed with the aqueous layer of this buffer in anaerobic conditions and the product was analyzed by GC-MS (S.I., Figure S.2). The ratio of the peak height of ¹⁸O included product and ¹⁶O included product, normalized to 100%, is reported as the percentage of ¹⁸O inclusion into the products.

5.6. Estimation of the Turnover Number (TON). The amount of oxidized product was determined by GC. To do that, the areas of the peaks of pure samples of different known concentrations were determined and plotted against the concentration of these samples. This plot is used as the calibration plot for that sample (S.I., Figure S.9). The amount of the oxidized product in the mixture was quantified by using respective calibration plots. CV experiments, done in anaerobic conditions, were used to calculate the amount of catalyst on the electrode surface. The ratio of the number of moles of product formed and the number of moles of catalyst (obtained from integration of the area under the CV response) depicts the turnover number (TON). Turnover frequency (TOF) is the TON divided by the run time in second (15 min = 900 s). TOF does not depict the initial rate; rather, it is the rate averaged over the entire duration of the reaction.

5.7. Estimation of the Faradaic Yield (FY). The moles of product produced per moles of electron, normalized to 100%, can be used as a parameter for quantifying the faradaic yield (FY) of the reaction. Thus, a 100% faradaic efficiency corresponds to 1 mol of product obtained for two moles of electron and one mole of oxygen (mono-oxygenase). The number of moles of electron consumed was quantified by calculating the total charge during the electrolysis. The following formula was used to calculate the FY.

$$FY = \frac{100 * \text{number of moles of product} * 2e^- * 96496}{\text{amount of charge accumulated}}$$

5.8. Estimation of the Kinetic Isotope Effect (KIE) and Solvent Kinetic Isotope Effect (SKIE). To measure the KIE for cyclohexane hydroxylation, cyclohexane-*d*₁₂ was used as the substrate. The deuterated substrate was dissolved in buffer, and electrolysis was performed as mentioned above with thiolate ligated FePf (S.I., Figure S.10.A). For KSIE measurement instead of pH 7, phosphate buffer pD 7 buffer with the same concentration of electrolyte was used, and substrates were saturated in this buffer to perform the electrochemical experiments with thiolate ligated FePf. In both the cases, products were quantified by GC-MS, and then the amount was compared with the product obtained for substrates stated above (S.I., Figure S.10.B).

5.9. Safety Statement. No unexpected or unusually high safety hazards were encountered.

■ ASSOCIATED CONTENT

📄 Supporting Information

The Supporting Information is available free of charge on the ACS Publications website at DOI: 10.1021/acscentsci.9b00046.

Characterization of the electrode, CV and XPS data, CO inhibition (Figure S.11) GC traces of the oxidized products and mass distribution spectra of the ¹⁸O labeled products (PDF)

■ AUTHOR INFORMATION

Corresponding Author

*Address: Department of Inorganic Chemistry, Indian Association for the Cultivation of Science, 2A&2B Raja SC Mullick Road, Jadavpur, Kolkata, West Bengal, India 700032. E-mail: abbeyde@gmail.com.

ORCID

Manjistha Mukherjee: 0000-0001-6550-6262

Abhishek Dey: 0000-0002-9166-3349

Notes

The authors declare no competing financial interest.

■ ACKNOWLEDGMENTS

This work was funded by the Department of Science and Technology, India, Grant EMR/2016/008063. M.M. acknowledges the integrated Ph.D. program of IACS. M.M. also acknowledges Dr. Kushal Sengupta and Dr. Sudipta Chatterjee for their guidance and Mr. Abhijit Nayek for providing the precursor complex for the preparation of FehPf. A.D. acknowledges Prof. Harry B. Gray for his valuable suggestions on the manuscript.

■ REFERENCES

- (1) Que, L., Jr; Tolman, W. B. Biologically inspired oxidation catalysis. *Nature* **2008**, *455*, 333.
- (2) Chen, M. S.; White, M. C. A Predictably Selective Aliphatic C–H Oxidation Reaction for Complex Molecule Synthesis. *Science* **2007**, *318*, 783.
- (3) Costas, M.; Mehn, M. P.; Jensen, M. P.; Que, L. Dioxygen Activation at Mononuclear Nonheme Iron Active Sites: Enzymes, Models, and Intermediates. *Chem. Rev.* **2004**, *104*, 939–986.
- (4) Garcia-Bosch, I.; Ribas, X.; Costas, M. Electrophilic Arene Hydroxylation and Phenol O–H Oxidations Performed by an Unsymmetric μ - η 1: η 1-O₂-Peroxo Dicopper(II) Complex. *Chem. - Eur. J.* **2012**, *18*, 2113–2122.
- (5) Baglia, R. A.; Zaragoza, J. P. T.; Goldberg, D. P. Biomimetic Reactivity of Oxygen-Derived Manganese and Iron Porphyrinoid Complexes. *Chem. Rev.* **2017**, *117*, 13320–13352.
- (6) Huang, X.; Groves, J. T. Oxygen Activation and Radical Transformations in Heme Proteins and Metalloporphyrins. *Chem. Rev.* **2018**, *118*, 2491–2553.
- (7) Nam, W. Synthetic Mononuclear Nonheme Iron–Oxygen Intermediates. *Acc. Chem. Res.* **2015**, *48*, 2415–2423.
- (8) Meunier, B. Metalloporphyrins as versatile catalysts for oxidation reactions and oxidative DNA cleavage. *Chem. Rev.* **1992**, *92*, 1411–1456.
- (9) Ortiz de Montellano, P. R. Hydrocarbon Hydroxylation by Cytochrome P450 Enzymes. *Chem. Rev.* **2010**, *110*, 932–948.
- (10) Poulos, T. L.; Johnson, E. F. Structures of Cytochrome P450 Enzymes. In *Cytochrome P450: Structure, Mechanism, and Biochemistry*;

Ortiz de Montellano, P. R., Ed.; Springer US: Boston, MA, 2005; pp 87–114.

(11) Denisov, I. G.; Makris, T. M.; Sligar, S. G.; Schlichting, I. Structure and Chemistry of Cytochrome P450. *Chem. Rev.* **2005**, *105*, 2253–2278.

(12) Schomburg, D.; Stephan, D. Indole 2,3-dioxygenase. In *Enzyme Handbook: Class 1.13–1.97: Oxidoreductases*; Schomburg, D., Stephan, D., Eds.; Springer: Berlin, 1994; pp 81–85.

(13) Ishida, T.; Kita, A.; Miki, K.; Nozaki, M.; Horiike, K. Structure and reaction mechanism of catechol 2,3-dioxygenase (metapyrocatechase). *Int. Congr. Ser.* **2002**, *1233*, 213–220.

(14) Wang, V. C. C.; Maji, S.; Chen, P. P. Y.; Lee, H. K.; Yu, S. S. F.; Chan, S. I. Alkane Oxidation: Methane Monooxygenases, Related Enzymes, and Their Biomimetics. *Chem. Rev.* **2017**, *117*, 8574–8621.

(15) Lange, S. J.; Que, L. Oxygen activating nonheme iron enzymes. *Curr. Opin. Chem. Biol.* **1998**, *2*, 159–172.

(16) Bugg, T. D. H.; Ramaswamy, S. Non-heme iron-dependent dioxygenases: unravelling catalytic mechanisms for complex enzymatic oxidations. *Curr. Opin. Chem. Biol.* **2008**, *12*, 134–140.

(17) Broderick, J. B. Catechol dioxygenases. *Essays Biochem.* **1999**, *34*, 173.

(18) Colabroy, K. L.; Zhai, H.; Li, T.; Ge, Y.; Zhang, Y.; Liu, A.; Ealick, S. E.; McLafferty, F. W.; Begley, T. P. The Mechanism of Inactivation of 3-Hydroxyanthranilate-3,4-dioxygenase by 4-Chloro-3-hydroxyanthranilate. *Biochemistry* **2005**, *44*, 7623–7631.

(19) Lara, M.; Mutti, F. G.; Glueck, S. M.; Kroutil, W. Oxidative Enzymatic Alkene Cleavage: Indications for a Nonclassical Enzyme Mechanism. *J. Am. Chem. Soc.* **2009**, *131*, 5368–5369.

(20) Steiner, R. A.; Kalk, K. H.; Dijkstra, B. W. Anaerobic enzyme-substrate structures provide insight into the reaction mechanism of the copper-dependent quercetin 2,3-dioxygenase. *Proc. Natl. Acad. Sci. U. S. A.* **2002**, *99*, 16625–16630.

(21) Oloo, W. N.; Que, L. Bioinspired Nonheme Iron Catalysts for C–H and C=C Bond Oxidation: Insights into the Nature of the Metal-Based Oxidants. *Acc. Chem. Res.* **2015**, *48*, 2612–2621.

(22) Que, L. The Road to Non-Heme Oxoferryls and Beyond. *Acc. Chem. Res.* **2007**, *40*, 493–500.

(23) Nam, W. High-Valent Iron(IV)–Oxo Complexes of Heme and Non-Heme Ligands in Oxygenation Reactions. *Acc. Chem. Res.* **2007**, *40*, 522–531.

(24) Shaik, S.; Kumar, D.; de Visser, S. P.; Altun, A.; Thiel, W. Theoretical Perspective on the Structure and Mechanism of Cytochrome P450 Enzymes. *Chem. Rev.* **2005**, *105*, 2279–2328.

(25) Shan, X.; Que, L. High-valent nonheme iron-oxo species in biomimetic oxidations. *J. Inorg. Biochem.* **2006**, *100*, 421–433.

(26) Sligar, S. G.; Makris, T. M.; Denisov, I. G. Thirty years of microbial P450 monooxygenase research: Peroxo-heme intermediates—The central bus station in heme oxygenase catalysis. *Biochem. Biophys. Res. Commun.* **2005**, *338*, 346–354.

(27) Schlichting, I.; Berendzen, J.; Chu, K.; Stock, A. M.; Maves, S. A.; Benson, D. E.; Sweet, R. M.; Ringe, D.; Petsko, G. A.; Sligar, S. G. The Catalytic Pathway of Cytochrome P450cam at Atomic Resolution. *Science* **2000**, *287*, 1615.

(28) Denisov, I. G.; Hung, S.-C.; Weiss, K. E.; McLean, M. A.; Shiro, Y.; Park, S.-Y.; Champion, P. M.; Sligar, S. G. Characterization of the oxygenated intermediate of the thermophilic cytochrome P450 CYP119. *J. Inorg. Biochem.* **2001**, *87*, 215–226.

(29) Davydov, R.; Makris, T. M.; Kofman, V.; Werst, D. E.; Sligar, S. G.; Hoffman, B. M. Hydroxylation of Camphor by Reduced Oxy-Cytochrome P450cam: Mechanistic Implications of EPR and ENDOR Studies of Catalytic Intermediates in Native and Mutant Enzymes. *J. Am. Chem. Soc.* **2001**, *123*, 1403–1415.

(30) Rittle, J.; Green, M. T. Cytochrome P450 Compound I: Capture, Characterization, and C–H Bond Activation Kinetics. *Science* **2010**, *330*, 933.

(31) Wallar, B. J.; Lipscomb, J. D. Dioxygen Activation by Enzymes Containing Binuclear Non-Heme Iron Clusters. *Chem. Rev.* **1996**, *96*, 2625–2658.

(32) Que, L.; Ho, R. Y. N. Dioxygen Activation by Enzymes with Mononuclear Non-Heme Iron Active Sites. *Chem. Rev.* **1996**, *96*, 2607–2624.

(33) Krest, C. M.; Onderko, E. L.; Yosca, T. H.; Calixto, J. C.; Karp, R. F.; Livada, J.; Rittle, J.; Green, M. T. Reactive Intermediates in Cytochrome P450 Catalysis. *J. Biol. Chem.* **2013**, *288*, 17074–17081.

(34) Kang, Y.; Chen, H.; Jeong, Y. J.; Lai, W.; Bae, E. H.; Shaik, S.; Nam, W. Enhanced Reactivities of Iron(IV)–Oxo Porphyrin π -Cation Radicals in Oxygenation Reactions by Electron-Donating Axial Ligands. *Chem. - Eur. J.* **2009**, *15*, 10039–10046.

(35) Hirao, H.; Que, L.; Nam, W.; Shaik, S. A Two-State Reactivity Rationale for Counterintuitive Axial Ligand Effects on the C–H Activation Reactivity of Nonheme FeIV = O Oxidants. *Chem. - Eur. J.* **2008**, *14*, 1740–1756.

(36) Kumar, D.; de Visser, S. P.; Sharma, P. K.; Derat, E.; Shaik, S. The intrinsic axial ligand effect on propene oxidation by horseradish peroxidase versus cytochrome P450 enzymes. *JBIC, J. Biol. Inorg. Chem.* **2005**, *10*, 181–189.

(37) de Visser, S. P.; Latifi, R.; Tahsini, L.; Nam, W. The Axial Ligand Effect on Aliphatic and Aromatic Hydroxylation by Non-heme Iron(IV)–oxo Biomimetic Complexes. *Chem. - Asian J.* **2011**, *6*, 493–504.

(38) Shaik, S.; Hirao, H.; Kumar, D. Reactivity of High-Valent Iron–Oxo Species in Enzymes and Synthetic Reagents: A Tale of Many States. *Acc. Chem. Res.* **2007**, *40*, 532–542.

(39) Gross, Z. The effect of axial ligands on the reactivity and stability of the oxoferryl moiety in model complexes of Compound I of heme-dependent enzymes. *JBIC, J. Biol. Inorg. Chem.* **1996**, *1*, 368–371.

(40) Sastri, C. V.; Lee, J.; Oh, K.; Lee, Y. J.; Lee, J.; Jackson, T. A.; Ray, K.; Hirao, H.; Shin, W.; Halfen, J. A.; Kim, J.; Que, L.; Shaik, S.; Nam, W. Axial ligand tuning of a nonheme iron(IV)–oxo unit for hydrogen atom abstraction. *Proc. Natl. Acad. Sci. U. S. A.* **2007**, *104*, 19181–19186.

(41) Guengerich, F. P.; Johnson, W. W. Kinetics of Ferric Cytochrome P450 Reduction by NADPH–Cytochrome P450 Reductase: Rapid Reduction in the Absence of Substrate and Variations among Cytochrome P450 Systems. *Biochemistry* **1997**, *36*, 14741–14750.

(42) Ferguson-Miller, S.; Babcock, G. T. Heme/Copper Terminal Oxidases. *Chem. Rev.* **1996**, *96*, 2889–2908.

(43) Sono, M.; Roach, M. P.; Coulter, E. D.; Dawson, J. H. Heme-Containing Oxygenases. *Chem. Rev.* **1996**, *96*, 2841–2888.

(44) Traylor, T. G. Synthetic model compounds for hemoproteins. *Acc. Chem. Res.* **1981**, *14*, 102–109.

(45) Collman, J. P. Synthetic models for the oxygen-binding hemoproteins. *Acc. Chem. Res.* **1977**, *10*, 265–272.

(46) Koval, I. A.; Gamez, P.; Belle, C.; Selmececi, K.; Reedijk, J. Synthetic models of the active site of catechol oxidase: mechanistic studies. *Chem. Soc. Rev.* **2006**, *35*, 814–840.

(47) Tani, F.; Matsu-ura, M.; Nakayama, S.; Naruta, Y. Synthetic models for the active site of cytochrome P450. *Coord. Chem. Rev.* **2002**, *226*, 219–226.

(48) Groves, J. T.; Han, Y.-Z. Models and Mechanisms of Cytochrome P450 Action. In *Cytochrome P450: Structure, Mechanism, and Biochemistry*; de Montellano, P. R. O., Ed.; Springer US: Boston, MA, 1995; pp 3–48.

(49) Dey, A.; Dey, S. G. CHAPTER 9 Model Compounds for Nitric Oxide Reductase. In *Metalloenzymes in Denitrification: Applications and Environmental Impacts*; The Royal Society of Chemistry, 2017; pp 185–224.

(50) Ozaki, S.-i.; Roach, M. P.; Matsui, T.; Watanabe, Y. Investigations of the Roles of the Distal Heme Environment and the Proximal Heme Iron Ligand in Peroxide Activation by Heme Enzymes via Molecular Engineering of Myoglobin. *Acc. Chem. Res.* **2001**, *34*, 818–825.

(51) Egawa, T.; Shimada, H.; Ishimura, Y. Formation of Compound I in the Reaction of Native Myoglobins with Hydrogen Peroxide. *J. Biol. Chem.* **2000**, *275*, 34858–34866.

- (52) Matsui, T.; Ozaki, S.-i.; Watanabe, Y. Formation and Catalytic Roles of Compound I in the Hydrogen Peroxide-Dependent Oxidations by His64 Myoglobin Mutants. *J. Am. Chem. Soc.* **1999**, *121*, 9952–9957.
- (53) Groves, J. T.; Watanabe, Y. Reactive iron porphyrin derivatives related to the catalytic cycles of cytochrome P-450 and peroxidase. Studies of the mechanism of oxygen activation. *J. Am. Chem. Soc.* **1988**, *110*, 8443–8452.
- (54) Pistorio, B. J.; Chang, C. J.; Nocera, D. G. A Phototriggered Molecular Spring for Aerobic Catalytic Oxidation Reactions. *J. Am. Chem. Soc.* **2002**, *124*, 7884–7885.
- (55) Rosenthal, J.; Luckett, T. D.; Hodgkiss, J. M.; Nocera, D. G. Photocatalytic Oxidation of Hydrocarbons by a Bis-iron(III)- μ -oxo Pacman Porphyrin Using O₂ and Visible Light. *J. Am. Chem. Soc.* **2006**, *128*, 6546–6547.
- (56) Bryliakov, K. P. Catalytic Asymmetric Oxygenations with the Environmentally Benign Oxidants H₂O₂ and O₂. *Chem. Rev.* **2017**, *117*, 11406–11459.
- (57) Rosenthal, J.; Nocera, D. G. Oxygen Activation Chemistry of Pacman and Hangman Porphyrin Architectures Based on Xanthene and Dibenzofuran Spacers. In *Prog. Inorg. Chem.*; John Wiley & Sons, Inc., 2007; pp 483–544.
- (58) Tabor, E.; Poltowicz, J.; Pamin, K.; Basag, S.; Kubiak, W. Influence of substituents in meso-aryl groups of iron μ -oxo porphyrins on their catalytic activity in the oxidation of cycloalkanes. *Polyhedron* **2016**, *119*, 342–349.
- (59) Guo, C.-C.; Liu, X.-Q.; Liu, Q.; Liu, Y.; Chu, M.-F.; Lin, W.-Y. First industrial-scale biomimetic oxidation of hydrocarbon with air over metalloporphyrins as cytochrome P-450 monooxygenase model and its mechanistic studies. *J. Porphyrins Phthalocyanines* **2009**, *13*, 1250–1254.
- (60) Hu, B.; Zhou, W.; Ma, D.; Liu, Z. Metallo-deuteroporphyryns as catalysts for the oxidation of cyclohexane with air in the absence of additives and solvents. *Catal. Commun.* **2008**, *10*, 83–85.
- (61) Zhou, X.; Ji, H. Biomimetic kinetics and mechanism of cyclohexene epoxidation catalyzed by metalloporphyrins. *Chem. Eng. J.* **2010**, *156*, 411–417.
- (62) Li, Y.; Zhou, X.; Chen, S.; Luo, R.; Jiang, J.; Liang, Z.; Ji, H. Direct aerobic liquid phase epoxidation of propylene catalyzed by Mn(III) porphyrin under mild conditions: evidence for the existence of both peroxide and Mn(IV)-oxo species from in situ characterizations. *RSC Adv.* **2015**, *5*, 30014–30020.
- (63) Zhao, M.; Wu, C.-D. Synthesis and post-metallation of a covalent-porphyrinic framework for highly efficient aerobic epoxidation of olefins. *Catal. Commun.* **2017**, *99*, 146–149.
- (64) Beyzavi, M. H.; Vermeulen, N. A.; Howarth, A. J.; Tussupbayev, S.; League, A. B.; Schweitzer, N. M.; Gallagher, J. R.; Platero-Prats, A. E.; Hafezi, N.; Sarjeant, A. A.; Miller, J. T.; Chapman, K. W.; Stoddart, J. F.; Cramer, C. J.; Hupp, J. T.; Farha, O. K. A Hafnium-Based Metal–Organic Framework as a Nature-Inspired Tandem Reaction Catalyst. *J. Am. Chem. Soc.* **2015**, *137*, 13624–13631.
- (65) Tabushi, I.; Yazaki, A. P-450-type dioxygen activation using hydrogen/colloidal platinum as an effective electron donor. *J. Am. Chem. Soc.* **1981**, *103*, 7371–7373.
- (66) Collman, J. P.; Dey, A.; Decreau, R. A.; Yang, Y.; Hosseini, A.; Solomon, E. I.; Eberspacher, T. A. Interaction of nitric oxide with a functional model of cytochrome c oxidase. *Proc. Natl. Acad. Sci. U. S. A.* **2008**, *105*, 9892–9896.
- (67) Collman, J. P.; Decreau, R. A.; Sunderland, C. J. Single-turnover intermolecular reaction between a Fe-superoxide-Cu cytochrome c oxidase model and exogenous Tyr244 mimics. *Chem. Commun.* **2006**, 3894–3896.
- (68) Fontecave, M.; Mansuy, D. Monooxygenase-like oxidations of olefins and alkanes catalyzed by manganese porphyrins: comparison of systems involving either O₂ and ascorbate or iodossylbenzene. *Tetrahedron* **1984**, *40*, 4297–4311.
- (69) Sengupta, K.; Chatterjee, S.; Dey, A. Catalytic H₂O₂ Disproportionation and Electrocatalytic O₂ Reduction by a Functional Mimic of Heme Catalase: Direct Observation of Compound 0 and Compound I in Situ. *ACS Catal.* **2016**, *6*, 1382–1388.
- (70) Sengupta, K.; Chatterjee, S.; Samanta, S.; Dey, A. Direct observation of intermediates formed during steady-state electrocatalytic O₂ reduction by iron porphyrins. *Proc. Natl. Acad. Sci. U. S. A.* **2013**, *110*, 8431–8436.
- (71) Sengupta, K.; Chatterjee, S.; Samanta, S.; Bandyopadhyay, S.; Dey, A. Resonance Raman and Electrocatalytic Behavior of Thiolate and Imidazole Bound Iron Porphyrin Complexes on Self Assembled Monolayers: Functional Modeling of Cytochrome P450. *Inorg. Chem.* **2013**, *52*, 2000–2014.
- (72) Chatterjee, S.; Sengupta, K.; Mondal, B.; Dey, S.; Dey, A. Factors Determining the Rate and Selectivity of 4e⁻/4H⁺ Electrocatalytic Reduction of Dioxygen by Iron Porphyrin Complexes. *Acc. Chem. Res.* **2017**, *50*, 1744–1753.
- (73) Dey, S.; Mondal, B.; Chatterjee, S.; Rana, A.; Amanullah, S.; Dey, A. Molecular electrocatalysts for the oxygen reduction reaction. *Nature Reviews Chemistry* **2017**, *1*, 0098.
- (74) Devaraj, N. K.; Decreau, R. A.; Ebina, W.; Collman, J. P.; Chidsey, C. E. D. Rate of Interfacial Electron Transfer through the 1,2,3-Triazole Linkage. *J. Phys. Chem. B* **2006**, *110*, 15955–15962.
- (75) Smalley, J. F.; Feldberg, S. W.; Chidsey, C. E. D.; Linford, M. R.; Newton, M. D.; Liu, Y.-P. The Kinetics of Electron Transfer Through Ferrocene-Terminated Alkanethiol Monolayers on Gold. *J. Phys. Chem.* **1995**, *99*, 13141–13149.
- (76) Love, J. C.; Estroff, L. A.; Kriebel, J. K.; Nuzzo, R. G.; Whitesides, G. M. Self-Assembled Monolayers of Thiolates on Metals as a Form of Nanotechnology. *Chem. Rev.* **2005**, *105*, 1103–1170.
- (77) Sengupta, K.; Chatterjee, S.; Samanta, S.; Dey, A. Direct observation of intermediates formed during steady-state electrocatalytic O₂ reduction by iron porphyrins. *Proc. Natl. Acad. Sci. U. S. A.* **2013**, *110*, 8431.
- (78) Hashimoto, S.; Tatsuno, Y.; Kitagawa, T. Resonance Raman Evidence for Oxygen Exchange between the Fe^{IV}=O Heme and Bulk Water during Enzymic Catalysis of Horseradish Peroxidase and Its Relation with the Heme-Linked Ionization. *Proc. Natl. Acad. Sci. U. S. A.* **1986**, *83*, 2417–2421.
- (79) Yoshimoto, F. K.; Guengerich, F. P. Mechanism of the Third Oxidative Step in the Conversion of Androgens to Estrogens by Cytochrome P450 19A1 Steroid Aromatase. *J. Am. Chem. Soc.* **2014**, *136*, 15016–15025.
- (80) Costas, M.; Chen, K.; Que, L. Biomimetic nonheme iron catalysts for alkane hydroxylation. *Coord. Chem. Rev.* **2000**, *200*–202, 517–544.
- (81) Groves, J. T.; Nemo, T. E. Aliphatic hydroxylation catalyzed by iron porphyrin complexes. *J. Am. Chem. Soc.* **1983**, *105*, 6243–6248.
- (82) Melander, L. C. S.; Saunders, W. H. *Reaction Rates of Isotopic Molecules*; Wiley: New York, 1980.
- (83) Bockrath, B. C.; Bittner, E. W.; Marecic, T. C. Kinetic isotope effects in hydrogen atom transfer reactions between benzylic carbons. *J. Org. Chem.* **1986**, *51*, 15–19.
- (84) Guengerich, F. P.: Chapter Nine - Kinetic Deuterium Isotope Effects in Cytochrome P450 Reactions. In *Methods in Enzymology*; Harris, M. E., Anderson, V. E., Eds.; Academic Press, 2017; Vol. 596; pp 217–238.
- (85) Miwa, G. T.; Walsh, J. S.; Kedderis, G. L.; Hollenberg, P. F. The use of intramolecular isotope effects to distinguish between deprotonation and hydrogen atom abstraction mechanisms in cytochrome P-450- and peroxidase-catalyzed N-demethylation reactions. *J. Biol. Chem.* **1983**, *258*, 14445–14449.
- (86) Guengerich, F. P. Kinetic Deuterium Isotope Effects in Cytochrome P450 Oxidation Reactions. *J. Labelled Compd. Radiopharm.* **2013**, *56*, 428–431.
- (87) Chowdhury, G.; Calcutt, M. W.; Guengerich, F. P. Oxidation of N-Nitrosoalkylamines by Human Cytochrome P450 2A6: Sequential Oxidation to Aldehydes and Carboxylic Acids and Analysis of Reaction Steps. *J. Biol. Chem.* **2010**, *285*, 8031–8044.
- (88) Gregory, M. C.; Denisov, I. G.; Grinkova, Y. V.; Khatri, Y.; Sliagar, S. G. Kinetic Solvent Isotope Effect in Human P450 CYP17A1-

Mediated Androgen Formation: Evidence for a Reactive Peroxoanion Intermediate. *J. Am. Chem. Soc.* **2013**, *135*, 16245–16247.

(89) Chatterjee, S.; Sengupta, K.; Samanta, S.; Das, P. K.; Dey, A. Concerted Proton–Electron Transfer in Electrocatalytic O₂ Reduction by Iron Porphyrin Complexes: Axial Ligands Tuning H/D Isotope Effect. *Inorg. Chem.* **2015**, *54*, 2383–2392.

(90) Vidakovic, M.; Sligar, S. G.; Li, H.; Poulos, T. L. Understanding the Role of the Essential Asp251 in Cytochrome P450cam Using Site-Directed Mutagenesis, Crystallography, and Kinetic Solvent Isotope Effect. *Biochemistry* **1998**, *37*, 9211–9219.

(91) Gerber, N.; Sligar, S. A role for Asp-251 in cytochrome P-450cam oxygen activation. *J. Biol. Chem.* **1994**, *269*, 4260–4266.

(92) Green, M. T.; Dawson, J. H.; Gray, H. B. Oxoiron(IV) in Chloroperoxidase Compound II Is Basic: Implications for P450 Chemistry. *Science* **2004**, *304*, 1653.

(93) Hayashi, Y.; Yamazaki, I. The oxidation-reduction potentials of compound I/compound II and compound II/ferric couples of horseradish peroxidases A2 and C. *J. Biol. Chem.* **1979**, *254*, 9101–9106.

(94) Finklea, H. O.; Hanshew, D. D. Electron-transfer kinetics in organized thiol monolayers with attached pentaammine(pyridine) ruthenium redox centers. *J. Am. Chem. Soc.* **1992**, *114*, 3173–3181.

(95) Bandyopadhyay, S.; Rana, A.; Mitra, K.; Samanta, S.; Sengupta, K.; Dey, A. Effect of Axial Ligand, Spin State, and Hydrogen Bonding on the Inner-Sphere Reorganization Energies of Functional Models of Cytochrome P450. *Inorg. Chem.* **2014**, *53*, 10150–10158.

(96) Chatterjee, S.; Sengupta, K.; Samanta, S.; Das, P. K.; Dey, A. Electrocatalytic O₂ Reduction Reaction by Synthetic Analogues of Cytochrome P450 and Myoglobin: In-Situ Resonance Raman and Dynamic Electrochemistry Investigations. *Inorg. Chem.* **2013**, *52*, 9897–9907.

(97) Collman, J. P.; Gagne, R. R.; Reed, C.; Halbert, T. R.; Lang, G.; Robinson, W. T. Picket fence porphyrins. Synthetic models for oxygen binding hemoproteins. *J. Am. Chem. Soc.* **1975**, *97*, 1427–1439.

(98) Qiang Feng, Z.; Imabayashi, S.; Kakiuchi, T.; Niki, K. Long-range electron-transfer reaction rates to cytochrome c across long- and short-chain alkanethiol self-assembled monolayers: Electroreflectance studies. *J. Chem. Soc., Faraday Trans.* **1997**, *93*, 1367–1370.